J Neurophysiol 109: 2086–2096, 2013.
First published January 23, 2013; doi:10.1152/jn.00907.2012.

Frequency-specific adaptation in human auditory cortex depends on the spectral variance in the acoustic stimulation

Björn Herrmann, Molly J. Henry, and Jonas Obleser
Max Planck Research Group "Auditory Cognition," Max Planck Institute for Human Cognitive and Brain Sciences, Leipzig, Germany

Submitted 15 October 2012; accepted in final form 20 January 2013

Herrmann B, Henry MJ, Obleser J. Frequency-specific adaptation in human auditory cortex depends on the spectral variance in the acoustic stimulation. *J Neurophysiol* 109: 2086–2096, 2013. First published January 23, 2013; doi:10.1152/jn.00907.2012.—In auditory cortex, activation and subsequent adaptation is strongest for regions responding best to a stimulated tone frequency and less for regions responding best to other frequencies. Previous attempts to characterize the spread of neural adaptation in humans investigated the auditory cortex N1 component of the event-related potentials. Importantly, however, more recent studies in animals show that neural response properties are not independent of the stimulation context. To link these findings in animals to human scalp potentials, we investigated whether contextual factors of the acoustic stimulation, namely, spectral variance, affect the spread of neural adaptation. Electroencephalograms were recorded while human participants listened to random tone sequences varying in spectral variance (narrow vs. wide). Spread of adaptation was investigated by modeling single-trial neural adaptation and subsequent recovery based on the spectro-temporal stimulation history. Frequency-specific neural responses were largest on the N1 component, and the modeled neural adaptation indices were strongly predictive of trial-by-trial amplitude variations. Yet the spread of adaption varied depending on the spectral variance in the stimulation, such that adaptation spread was broadened for tone sequences with wide spectral variance. Thus the present findings reveal context-dependent auditory cortex adaptation and point toward a flexibly adjusting auditory system that changes its response properties with the spectral requirements of the acoustic environment.

auditory cortex; frequency-specific adaptation; N1 component; short-term plasticity

ADAPTATION refers to the phenomenon by which the responsiveness of a neural population declines with sustained stimulation. In tonotopically organized regions, such as auditory cortex, this adaptation is frequency specific. That is, regions responding best to a particular tone frequency adapt most strongly, whereas those responding best to other frequencies adapt to a lesser degree (Jääskeläinen et al. 2011).

Much of the electroencephalographic (EEG) research on the neural mechanisms of auditory processing in humans has focused on the N1 component, a negative deflection of event-related potentials (ERPs) that is maximal around 80–120 ms after stimulus onset. The N1 is associated with basic auditory perception (for a review see Näätänen and Picton 1987), and its neural sources have been localized to auditory cortex (Maess et al. 2007; Pantev et al. 1988).

Using the N1 as a measure of auditory cortex activations, one line of research has focused on recovery from adaptation over time after activation (e.g., McEvoy et al. 1997; Rosburg et al. 2010; Sams et al. 1993). These studies revealed that the N1 amplitude increases with increasing time between two successive tone stimulations (i.e., with increasing onset-to-onset interval) and that the neural population asymptotically reapproaches full responsiveness after ~10 s.

Another line of research has focused on the frequency specificity of the N1 amplitude, showing that the presentation of a tone affects the responsiveness of the neural population responding to a succeeding tone. This influence increases with decreasing frequency separation between the two tones (e.g., Butler 1968; May et al. 1999; Näätänen et al. 1988). It should be noted that the term "frequency-specific adaptation" is potentially problematic when applied to a component of the evoked potential, here the N1. This is because the relationships between spiking behavior of single neurons, local field potentials, and human EEG are still not well understood (Buzsáki et al. 2012). Regardless of this, previous findings using N1 amplitude as a dependent measure were nevertheless taken as indices for neural adaptation spanning across a range of frequency-specific cortical regions in auditory cortex, and thereby affecting the N1 amplitude (Näätänen et al. 1988; Picton et al. 1978).

In addition, early studies suggested that the spread of frequency-specific neural adaptation underlying N1 amplitude variations is very broad (e.g., Butler 1968; Gorny and Butler 1975), whereas the adaptation spread reported in later studies varied extensively from the earlier studies (e.g., Näätänen et al. 1988). More recent findings, on the other hand, show that the response properties of neurons along the auditory pathway can change depending on the acoustic stimulation (e.g., Dahmen et al. 2008, 2010; Dean et al. 2005; Taaseh et al. 2011). For example, it has been suggested that individual neurons adapt to the variance as well as to the spectral properties of the acoustic stimulation (Bitterman et al. 2008; Dean et al. 2005). Such short-term plasticity in auditory cortex has been proposed as an important mechanism involved in a variety of cognitive and auditory stimulus processing phenomena (Jääskeläinen et al. 2007, 2011).

Here we aimed to link these previous findings from single-neuron recordings in animals to human scalp potentials. The present EEG study thus investigated frequency-specific adaptation in auditory cortex. Specifically, we asked whether the spread of N1 adaptation depends on contextual factors in the acoustic stimulation, here the spectral variance. To this end, random tones were presented in rapid sequences in which the frequency spacing between tones was varied. A simple computational model predicted trial-by-trial auditory cortex activations from the combination of spread of adaptation and recovery from adaptation. The results suggest short-term plastic

Address for reprint requests and other correspondence: B. Herrmann, Max Planck Research Group "Auditory Cognition," Max Planck Institute for Human Cognitive and Brain Sciences, Stephanstraße 1A, 04103 Leipzig, Germany (e-mail: bherrmann@cbs.mpg.de).

broadening of neural adaptation spread for stimulation sequences that are wide in spectral variance.

MATERIALS AND METHODS

Participants. Twenty normal-hearing participants aged 21–30 yr (mean 25 yr; 11 women, 9 men) took part in the experiment. They were all right-handed as measured by the Edinburgh Handedness Inventory (Oldfield 1971). Participants gave written informed consent prior to the experiment and were paid €7/h for their participation. The study was in accordance with the Declaration of Helsinki and approved by the local ethic committee of the University of Leipzig.

Stimuli. All stimulus materials were created in MATLAB (v. 7.11; applying the *vco.m* function) with a sampling rate of 44,100 Hz and 24-bit resolution. Stimuli consisted of three sets of eight logarithmically spaced sinusoidal tones that varied in frequency spacing (that is, in spectral variance) and center frequency (Fig. 1*A*): narrow low (spanning ~1 octave; 840, 920, 1,007, 1,103, 1,208, 1,323, 1,449, and 1,587 Hz), narrow high (also spanning ~1 octave; 1,103, 1,208, 1,323, 1,449, 1,587, 1,738, 1,903, and 2,084 Hz), and wide (spanning ~2 octaves; 700, 840, 1,007, 1,208, 1,449, 1,738, 2,084, and 2,500 Hz). Henceforth we refer to these three frequency spacings as spectral variance conditions. Tone duration was 200 ms, including 10-ms rise and fall times.

Deviant tones were constructed by inserting a 20-ms (5-ms rise and fall times) downward frequency excursion into the center of a tone with the MATLAB *vco.m* function. In brief, the *vco.m* function generates a sine wave and, at the same time, allows for time-sensitive frequency changes by manipulating the phase angles of the wave. The magnitude of the frequency excursion was estimated for each participant individually with psychophysical threshold estimation (see below).

Procedure. Acoustic stimulation and EEG recording were carried out in an electrically shielded and sound-attenuated booth. Participants were seated in a comfortable chair and watched a silent movie (no subtitles) of their choice throughout testing. Auditory stimuli were presented via headphones (Sennheiser HD 25-SP II) at 60 dB above the individual hearing threshold.

Each participant underwent the following procedure: First, hearing thresholds were determined with the method of limits for seven frequencies covering the range used in the experiment and were estimated for all frequencies with linear regression.

Second, participants performed an adaptive tracking procedure in order to establish individual detection thresholds for frequency excursions in deviant tones. A simple one-down one-up staircase method was implemented in order to estimate the frequency excursion yielding 50% detection (Leek 2001). This procedure was again completed for seven of the tone frequencies, and the thresholds were estimated for all frequencies with linear regression. Across participants, mean estimated thresholds ranged from 2.13% (range: 0.87–3.21%) for the 700-Hz tone to 1.24% (range: 0.78–2.00%) for the 2,500-Hz tone.

Third, in the main experiment, six blocks were presented (2 per spectral variance condition) while EEG was recorded. The order of spectral variance conditions was counterbalanced across participants. Each block started with a silent period of >10 s prior to the beginning of the acoustic stimulation to ensure full responsiveness of neural populations at block onset. Within each block, a train of 8 unique tones was presented 199 times without pauses between trains. Tone frequencies within each train were randomized (Fig. 1*B*). Tones containing a small frequency excursion (deviants) were randomly intermixed into the stimulation, with a minimum of 2 s and a maximum of 7 s between two deviant tones. No two consecutive tones ever had the same frequency, even during transitions between trains. Tones were presented with a comparably short onset-to-onset interval of 0.5 s. Overall, participants heard a total of 1,592 tones per block (199 for each of the 8 frequencies) including 176 deviant tones (11%) counterbalanced across tone frequencies.

We also employed an attention manipulation: In half of the blocks participants were instructed to ignore the acoustic stimulation, while in the other half of the blocks participants were instructed to complete a deviant-detection task that required participants to respond with a button press when they detected a deviant tone. In both task conditions, participants were instructed to visually monitor a silent movie. Ignore and attend blocks were presented in an alternating fashion with the starting condition counterbalanced across participants. In total, the experiment lasted ~3 h.

Behavioral data analysis. For each participant, the proportion of correctly detected deviant tones was calculated. A response was considered a hit (correct response) if the button press was made within 0.2–1 s after the onset of the frequency excursion defining the deviant.

An empirical guessing level was estimated for each participant in each block. The reason was that individual participants differed in their response biases (i.e., their willingness to indicate that they detected a deviant). Thus increased hit rates could have resulted from more liberal response biases, which would have in turn led to more button presses falling into the time window during which they were considered hits. Thus calculation of an empirical guessing rate accounted for individual response biases. The procedure was as follows: First, the total number of responses made within a block was calculated. Then, in a simulation, the same number of responses was randomly distributed across that block, assuming the same temporal location of all deviant stimuli. Next, the detection rate was calculated given the new dispersion of responses. This procedure was repeated 100,000 times, and the empirical guessing level was taken as the mean detection rate over iterations. Detection rates were tested statistically against empirical guessing rates to ensure that performance exceeded chance.

Detection rates were evaluated across the three spectral variance conditions by means of a two-way repeated-measures analysis of variance (rmANOVA), with the factors spectral variance (narrow low, narrow high, wide) and rate type (detection rate, guessing level). To correct for the nonnormality of [0;1]-bound proportion data before the

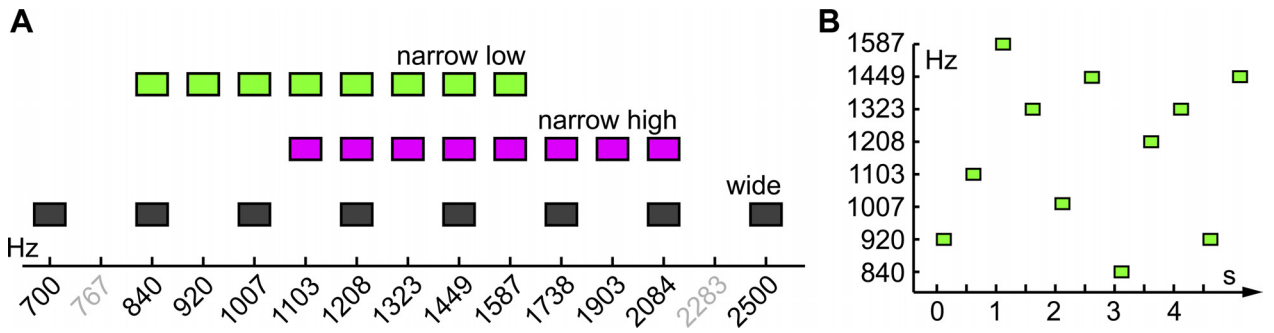

Fig. 1. Experimental design. *A*: 3 spectral variance conditions and their corresponding tone frequencies. Note that the frequency spacing is logarithmic (log2). *B*: example of the random tone presentation for the narrow low condition.

analysis, detection rates (hits and empirical guess rates) were transformed to rationalized arcsine units (rau; Studebaker 1985).

For all rmAONVAs conducted throughout the study, the Greenhouse-Geisser correction was applied whenever the assumption of sphericity was violated (according to Mauchly's criterion; Greenhouse and Geisser 1959). The original degrees of freedom are reported along with the ϵ correction coefficient and the corrected probability. Effect sizes are provided as generalized η^2 (η^2_G; Bakeman 2005).

EEG recording and data preprocessing. The EEG was recorded at a 500-Hz sampling rate and low-pass filtered online at 135 Hz (TMS international, Enschede, The Netherlands). Electrodes (Ag/Ag-Cl electrodes) were placed at the following positions (Easycap, Herrsching, Germany): Fp1, Fp2, Fz, F3, F4, F7, F8, FC3, FC4, FT7, FT8, Cz, C3, C4, T7, T8, CP5, CP6, Pz, P3, P4, P7, P8, O1, O2, the nose, and at the left (A1) and right (A2) mastoids. The nose served as online reference. The electrooculogram was recorded from vertical and horizontal bipolar montages to measure blinks and eye movements. The ground electrode was placed at the sternum, and impedances were kept below 5 kΩ for all electrodes.

Data analysis was carried out with FieldTrip software (**http://fieldtrip.fcdonders.nl/**; v20110527; Oostenveld et al. 2011) in combination with custom MATLAB scripts. EEG recordings were high-pass filtered off-line at 0.5 Hz (zero phase shift), re-referenced to the linked mastoids, low-pass filtered at 100 Hz (zero phase shift), and downsampled to 250 Hz. Re-referencing to the linked mastoids was done in order to gain better signal-to-noise ratio of N1 responses at fronto-central-parietal electrodes, at the expense of losing information about N1 polarity reversal at the mastoids. Recordings were divided into epochs of −1.6 to 1.9 s time-locked to the tone onset. Independent components analysis was used to correct for artifacts such as eye movements, electrical heart activity, and noisy channels. Subsequently, epochs were excluded if they contained a signal range larger than 120 μV in any of the EEG electrodes. Epochs were then filtered with a 20-Hz (zero phase shift) low pass and redefined for data analysis ranging from −0.1 to 0.4 s time-locked to the tone onset. Baseline correction was applied by subtracting the mean amplitude of the −0.1 to 0 s time window from the epoch.

EEG data analysis. In the present study we focused our examination on frequency-specific modulations of neural activations in the different spectral variance conditions. Hence, brain responses to deviant tones as well as brain responses to tones directly following deviant tones were excluded from the analysis to avoid contaminations arising from button press responses.

All statistical analyses were conducted for a fronto-central-parietal electrode cluster (Fz, F3, F4, FC3, FC4, Cz, C3, C4, Pz, P3, P4) showing the strongest responses in the ERP (see Fig. 3). This electrode cluster is also in strong agreement with previous studies investigating early event-related responses known to reflect auditory cortical responses (e.g., Hari et al. 1982; Näätänen et al. 1988). Time courses displayed in the figures reflect the average of these channels.

Note that the task manipulation (i.e., participants being instructed to ignore or to attend the stimuli) did not lead to any statistically significant effects in the EEG analyses. Thus ignore and attend conditions are pooled in the figures for display purposes. Nevertheless, analyses were conducted with the task factor included (if not stated otherwise), and the statistical results are provided for completeness.

EEG data analysis was twofold. First, responses to each of the eight unique tones in each spectral variance condition were averaged over tone presentations, and quadratic fits were conducted to assess the pattern of response magnitude as a function of tone frequency. Second, trial-by-trial frequency-specific variations in neural response magnitude were investigated with a simple computational model. The model accounts for neural adaptation spread along the tonotopic gradient of the auditory cortex as well as for recovery from adaptation after activation. The following sections describe both approaches in more detail.

Analysis of quadratic fits as a measure of global frequency-specific responses. In light of the tonotopic organization of auditory cortex, we hypothesized that regions responding best to frequencies close to the center of a spectral variance condition would become more adapted than regions responding best to tone frequencies at the edge of the condition, which are less repetitively coadapted. Thus mean response magnitudes were expected to be smallest for tone frequencies close to the center of a spectral variance condition and largest for tone frequencies at the edge (Ulanovsky et al. 2004).

To this end, quadratic fits were conducted to test for global effects of frequency specificity. We refer to this analysis as being an analysis of global frequency specificity, because it is based on the mean responses across a block of stimulation. In particular, for each of the three spectral variance conditions single-trial brain response time courses were averaged for each of the eight unique tone frequencies. Then, for each time point in the epoch (−0.1 to 0.4 s) and separately for each channel, a quadratic function was fitted to the mean response amplitudes as a function of frequency with a least-squares routine:

$$\mathbf{y} = b_2\mathbf{x}^2 + b_1\mathbf{x} + b_0$$

where $\boldsymbol{y}$ corresponds to the predicted response amplitudes, $\boldsymbol{x}$ to the unique tone frequencies of one spectral variance condition (log2 transformed and zero centered), and b to the estimated coefficients.

Important for the focus of the present study, the second-order b_2 coefficient directly reflects the tightness of the best-fit quadratic function, that is, the degree of frequency specificity. A value of $b_2 = 0$ would indicate the absence of frequency specificity, while a significant difference from 0 would indicate frequency-specific neural responses.

Thus, for the statistical analysis, individually estimated b_2 coefficients at each channel of the electrode cluster were averaged and then tested against zero with a paired-sample *t*-test at each time point. False discovery rate (FDR) correction was applied to account for multiple comparisons across time points (Benjamini and Hochberg 1995; Genovese et al. 2002).

To test for differences between spectral variance and task conditions, an rmANOVA was conducted for b_2 coefficients averaged within the N1 time window (0.08–0.12 s) in which the quadratic fit was significant for all spectral variance conditions (see below). The rmANOVA included the factors spectral variance (narrow low, narrow high, wide) and task (ignore, attend).

Timing of neural responses. N1 response latencies were analyzed to investigate whether the timing of the neural responses differed between spectral variance and task conditions. Brain responses were averaged across trials, channels, and the eight unique tone frequencies in each spectral variance condition. Analysis of response latencies was restricted to the overall N1 latency in the spectral variance conditions because individual peak latencies could not be estimated for the low-amplitude responses elicited by tone frequencies close to the center frequency. A simplified jackknifing procedure was applied to extract N1 latency estimates (Smulders 2010). These were then subjected to an rmANOVA comprising the factors spectral variance (narrow low, narrow high, wide) and task (ignore, attend).

A simple model of frequency-specific adaptation. To investigate frequency-specific response adaptation on a trial-by-trial basis, we calculated an index of expected neural adaptation at the time of each tone onset based on the history of presented tones (Fig. 2). With this analysis we aimed to explore a biologically meaningful estimate of adaptation spread for the neural population activated by the tones in the different spectral variance conditions.

To this end, we combined a decay function describing recovery from neural adaptation over time (Lu et al. 1992a, 1992b; Mäkelä et al. 1993; McEvoy et al. 1997; Sams et al. 1993) with a Gaussian function describing neural (co-)adaptation along the frequency gradient of the auditory cortex. A Gaussian function was chosen based on previous studies modeling tuning properties of auditory cortex neurons (e.g., Dahmen et al. 2008; Montgomery and Wehr 2010; Taaseh

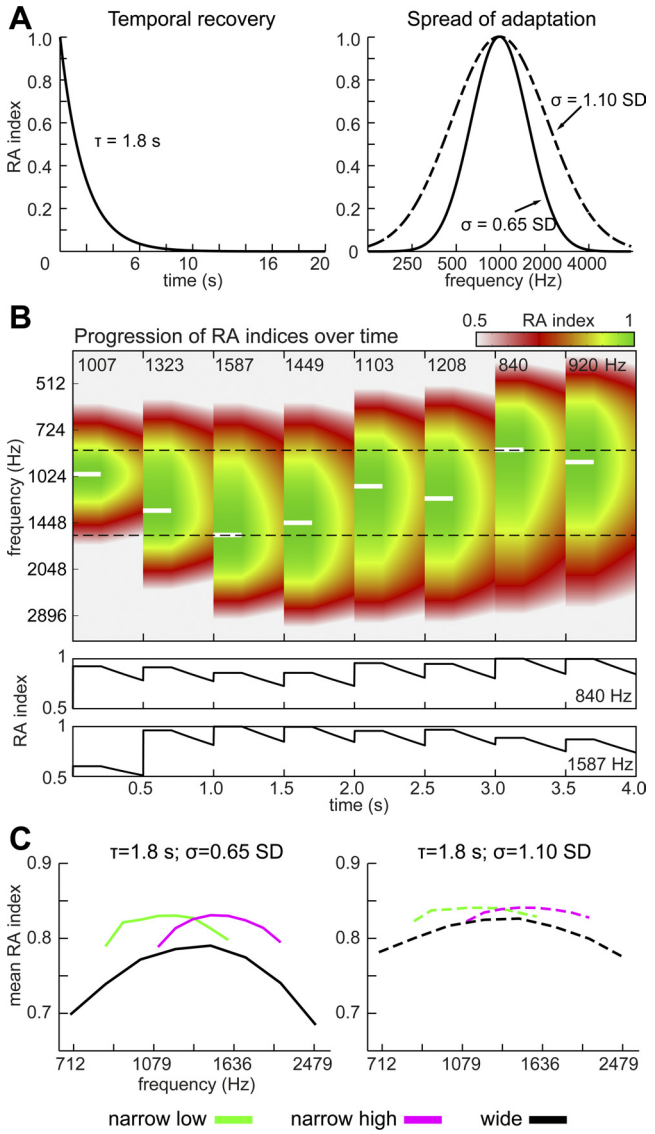

Fig. 2. Examples of the response adaptation (RA) index. *A*: main parameters of the RA model: exponential decay function for temporal recovery (τ, *left*) and Gaussian function for adaptation spread (σ, *right*). SD, standard deviation unit. *B*: example of RA indices over time for a sequence of tones in the narrow low condition (τ = 1.8 s; σ = 0.65 SD). *Top*: a tone of 0.2-s duration is presented every 0.5 s (*x*-axis). The presented tone frequencies are indicated by white lines and additionally written inside the graph. RA indices are color coded (green, full adaptation). At tone presentation, the corresponding frequency-specific cortical region and its neighboring regions adapt (*y*-axis; frequency gradient of the auditory cortex), i.e., RA indices increase at tone onset (according to the Gaussian function centered at the tone frequency that is presented) and decrease after tone offset (recovery). *Bottom*: time course of the RA index for 2 frequencies (840 Hz and 1,587 Hz, indicated by black dashed lines, *top*). *C*: mean RA index (tone-specific average across the block) for each spectral variance condition based on the random tone sequences presented to 1 participant. Two different widths (σ = 0.65 SD, solid lines; σ = 1.10 SD, dashed lines) are shown for a recovery time of τ = 1.8 s (see also Figs. 5 and 6). Note that for the whole figure lower RA indices correspond to larger expected response amplitudes.

et al. 2011) and is in line with the monotonic increase of the N1 amplitude with increasing frequency separation between two tones (May et al. 1999; Näätänen et al. 1988; Picton et al. 1978).

Here we calculated a normalized response adaptation (RA) index that ranged from 0 to 1, where 0 reflects no adaptation (i.e., full responsiveness) and 1 reflects full adaptation of the neural population. Calculation of the RA index for each trial was based on the individual sequence of tones presented to each participant, i.e., independent of the recorded brain data. Figure 2 gives a visual description of the model. Note that we use the term "adaptation" as the inverse to responsiveness, i.e., stronger adaptation relates to reduced responsiveness of the neural population and therefore to a reduced amplitude in the EEG.

Formally, the expected RA at each trial's tone onset was calculated with the following equations:

$$\mathbf{RA}_{:,j+1} = \mathbf{ma} \times e^{\frac{-\Delta t}{\tau}} \quad (1)$$

Here ***RA*** corresponds to an $n \times p$ response adaptation matrix. The matrix contains the expected adaptation for the neural populations along the tonotopic gradient of auditory cortex (rows) at each trial's tone onset (columns). That is, adaptation at each trial is tracked for the whole neural population stimulated in a given spectral variance condition (here n = 8, with n = number of unique tone frequencies in 1 spectral variance condition), in order to estimate the trial-by-trial adaptation spread influences. The variable j is the index of the trials ($j = 1 \ldots p$, with p = number of trials, i.e., 1,592), Δt is the time over which recovery takes place before the onset of the next tone (here set to the interstimulus interval of 0.3 s, i.e., recovery starts at tone offset), and τ is the decay in seconds. All entries in $\boldsymbol{RA}_{:,1}$ were set to 0, that is, at the first trial the auditory cortex is assumed to be not adapted, i.e., in a maximally responsive state.

The term ***ma*** is a vector comprising the momentary expected response adaptation for each unique tone frequency instantaneously after tone onset. We calculated ***ma*** by adding response adaptation and scaled responsiveness at trial j, according to the following equation:

$$\mathbf{ma} = \mathbf{RA}_{:,j} + \mathbf{a} \circ (1 - \mathbf{RA}_{:,j}) \quad (2)$$

where the operator o refers to an entrywise multiplication (Hadamard product) and ***a*** is a Gaussian function centered at the presented tone frequency f_i of trial j:

$$\mathbf{a} = e^{-0.5 \times \left(\frac{f - f_i}{\sigma}\right)^2} \quad (3)$$

In *Eq. 3*, ***f*** is the vector of the eight unique frequencies (log2 spaced) in a single spectral variance condition and σ describes the width of the Gaussian function, i.e., the spread of adaptation along the tonotopic gradient. The index i refers to the tone frequency presented on trial j, i.e., i is not an index incrementing from 1 to n but rather indexes the row entry in ***f*** and ***RA*** on trial j.

As a last step, the ***RA*** matrix was reduced to a vector comprising only the expected adaptation indices for the tone frequencies actually presented during the experiment and then further reduced to comprise only those values corresponding to the trials included in the analysis (i.e., excluding deviant trials and their successors as well as trials rejected as artifacts).

To summarize, the relevant parameters from the model are τ, which reflects the rate of recovery from adaptation (in s) and σ, which reflects the spread of adaptation along the frequency gradient of auditory cortex [in standard deviation units (SD)]. RA indices were calculated separately for all parameter combinations ranging from τ = 0.5 to 4.5 s (in steps of 0.1) and σ = 0.1 to 2.5 SD (in steps of 0.05). The other variables were predefined by the experimental setup.[1]

[1] Note that we did not calculate a RA that directly predicts the neural response magnitude in microvolts, where the parameters τ and σ would be estimated in a least-squares routine, because the parameters τ and σ are strongly inversely related (see Fig. 5). Furthermore, the equations to calculate RA would need to incorporate explicit variables for the minimum and maximum amplitudes. However, a measure of minimum amplitude was absent in the present experimental setup (and is in principle difficult to estimate). Importantly, the minimum amplitude could not be set to zero (as has been done implicitly in previous studies), because the averaged responses depicted in Fig. 3 already indicate that N1 amplitudes span from positive to negative microvolt values.

Single-trial EEG activation as a function of response adaptation index. The RA index model was used to predict the actual EEG data as follows. A linear function was fitted to single-trial neural response amplitudes as a function of RA index, separately for each combination of τ and σ parameters. The linear function was separately fitted for each time point and channel in each spectral variance and task condition. The first five trials of each block were discarded from the analysis in order to estimate the frequency-specific amplitude modulations over the block unbiased by the extreme values of the first trials, where there is only a little adaptation. This resulted in a unique slope and intercept value for each τ-σ parameter combination that described the correlation between RA index and brain activation magnitude. Slopes and intercepts were averaged across the channels of the electrode cluster.

The width σ of the Gaussian function (adaptation spread) best describing the observed N1 amplitude variations was then estimated for each τ independently. For each σ at a particular τ, the intercept of the linear fit directly reflects the predicted maximal N1 amplitude assuming no adaptation (RA index = 0), i.e., at full responsiveness. These intercepts were averaged within the N1 time window (0.08–0.12 s) as well as across task conditions (ignore, attend; pretests did not show any indication of differences between ignore and attend conditions). Then these averaged, predicted N1 amplitudes were compared to the maximal observed N1 amplitude, taken as the average across the first trial in each of the six blocks, i.e., the trials that followed a >10-s period of silence before the acoustic stimulation started. The σ for which the difference between the predicted and observed N1 amplitudes at no adaptation was minimum was then selected as the best fit to the data at a particular τ.

Four participants were excluded from subsequent analyses because the resulting σ from this minimization was at the boundary of the predefined range (σ = 0.1–2.5 SD). For the remaining 16 participants included in subsequent analyses, this led to one σ for each τ that best explained the amplitude data in the N1 time window.

Differences in τ were not expected, because the spectral variance of the stimulation was varied whereas the onset-to-onset interval was the same for all conditions. Thus statistical analyses were conducted for the individual σ estimates at a fixed τ of 1.8 s. This τ value was chosen on the basis of the observed overall recovery in Sams at al. (1993), which is also within the range of other previous estimations of τ (Lu et al. 1992a, 1992b; Mäkelä et al. 1993; McEvoy et al. 1997). A one-way rmANOVA comprising the factor spectral variance (narrow low, narrow high, wide) was carried out to examine differences in adaptation spread (σ) between spectral variance conditions.

Individual slope values from the linear fits (for individually estimated σ at τ = 1.8 s) were then statistically compared to zero in order to test whether the RA indices were predictive of the single-trial N1 amplitude variations. Differences between slope values in the different spectral variance conditions were assessed with a one-way rmANOVA with the factor spectral variance (narrow low, narrow high, wide).

Finally, based on the individually estimated σ at τ = 1.8 s, the slope values at each time point of the epoch were tested against zero with a paired-samples *t*-test in order to explore whether the RA index is also predictive of activation magnitude variations in time windows different from the N1 time window. FDR correction was applied to account for multiple comparisons across time points (Benjamini and Hochberg 1995; Genovese et al. 2002).

RESULTS

Behavioral results. The overall mean proportion correct was 0.46 (narrow low: 0.45 ± 0.04 SE; narrow high: 0.49 ± 0.04 SE; wide: 0.45 ± 0.04 SE). The rmANOVA conducted on the rau-transformed proportions revealed a main effect of rate type ($F_{1,19}$ = 213.46, $P < 0.001$, η^2_G = 0.341) caused by a larger proportion correct for the detection rate compared with the empirical guessing level, indicating that performance was better than chance (overall chance level: 0.11 ± 0.01 SE). No effect for spectral variance conditions ($F_{2,38}$ = 2.25, P = 0.119) and no spectral variance × rate type interaction was found ($F_{2,38}$ = 1.99, P = 0.151).

EEG results. Figure 3 shows time courses of the brain response to each unique tone frequency in the different spectral variance conditions. Visual inspection already indicates a strong modulation of the brain activation in the N1 time window. Bar graphs depict the frequency-specific brain activations in the N1 time window, in which mean amplitudes increase with increasing frequency distance to the center frequency of the spectral variance condition.

Analysis of quadratic fits indicates global frequency specificity. An analysis of quadratic fits was conducted to investigate response amplitude as a function frequency (i.e., frequency specificity) at each time point of the epoch. Importantly, mean amplitudes in this analysis were related to their respective tone frequencies in log2 space.

Figure 4*A* depicts the time course of b_2 coefficients from quadratic fits for each spectral variance condition. Note that b_2 values differing significantly from 0 reflect frequency-specific brain responses.

As indicated by the colored horizontal bars in Fig. 4*A*, quadratic coefficients (b_2) differed significantly from 0 in the N1 time window (0.08–0.12 s) in all spectral variance conditions. In this time window, mean brain responses were significantly modulated by the stimulated tone frequency, with smaller amplitudes elicited by tone frequencies close to the center frequency of a spectral variance condition compared with the tone frequencies at the edge. The topographical distributions of these effects showed centro-frontal maxima (Fig. 4*B*).

In general, quadratic fits in the N1 time window were similarly good in all three spectral variance conditions. Pairwise *t*-tests did not reveal any significant differences between the minimized root mean square error of approximation (for all, $P > 0.15$).

Next, we tested for differences in the tightness of the mean response function (i.e., quadratic coefficients) between spectral variance conditions. An rmANOVA was conducted for the 0.08–0.12 s time window, where all spectral variance conditions had shown significant frequency-specific effects. The rmANOVA revealed a main effect of spectral variance ($F_{2,38}$ = 34.92, $P < 0.001$, η^2_G = 0.122). Post hoc tests showed that the quadratic coefficients (b_2) for the wide condition were significantly smaller than for the two narrow conditions (narrow low: $F_{1,19}$ = 50.71, $P < 0.001$, η^2_G = 0.201; narrow high: $F_{1,19}$ = 47.92, $P < 0.001$, η^2_G = 0.193), which were not different from each other ($F_{1,19}$ = 0.15, P = 0.700). Thus the data reveal a broader response amplitude function for the wide compared with the narrow spectral variance conditions (Fig. 4*C*). Note that the main effect of task and the spectral variance × task interaction were not significant ($F_{1,19}$ = 0.08, P = 0.775 and $F_{2,38}$ = 0.38, P = 0.616, ϵ = 0.716, respectively).

To illustrate the predicted N1 amplitudes assuming fixed frequency specificity for narrow and wide conditions, the estimated coefficients from quadratic fits in the narrow conditions were used to predict N1 amplitudes in the wide condition. Specifically, estimated coefficients were averaged across narrow conditions, within the N1 time window, and also across the electrodes and participants. Mean coefficients were then used to predict the N1 amplitude at each tone frequency of the wide condition (Fig. 4*D*). This analysis shows that the N1 ampli-

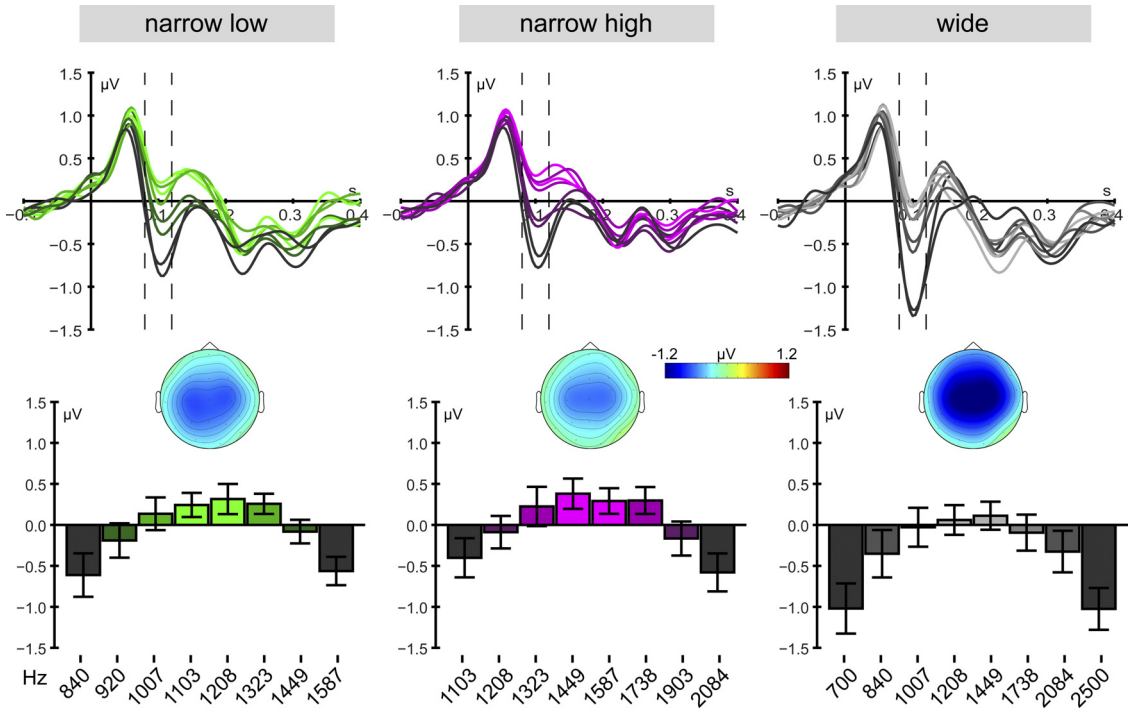

Fig. 3. Event-related potentials (ERPs) to the tones in each spectral variance condition (pooled across ignore and attend conditions). *Top*: response time courses for each tone frequency. *Bottom*: mean activation strength for the N1 time window (0.08–0.12 s, delimited with dashed lines in time courses). Topographies are shown for the N1, averaged across the 2 edge frequencies of each spectral variance condition. Note that for the N1 time window larger brain responses correspond to more negative amplitudes.

tudes in the wide condition were smaller than would be predicted under the assumption of fixed frequency specificity for narrow and wide conditions.

We also tested for linear changes in mean response amplitudes across frequencies by comparing the averaged linear coefficients (b_1) in the N1 time window against zero. There were no significant effects in any of the spectral variance conditions (all $P > 0.2$), thereby indicating the absence of a decrease or increase in amplitude with increasing tone frequencies.

Timing of brain responses. An rmANOVA was conducted to test for potential N1 latency differences between spectral variance and task conditions. There were no significant effects: spectral variance ($F_{2,38} = 0.97$, $P = 0.389$), task ($F_{1,19} < 0.01$, $P = 0.982$), spectral variance × task ($F_{2,38} = 0.02$, $P = 0.944$, $\epsilon = 0.653$).

Trial-by-trial frequency-specific brain activations reveal underlying adaptation spread. Trial-by-trial amplitude variations were investigated with a model of neural response adaptation (Fig. 2). Figure 5*A* depicts the mean adaptation spread param-

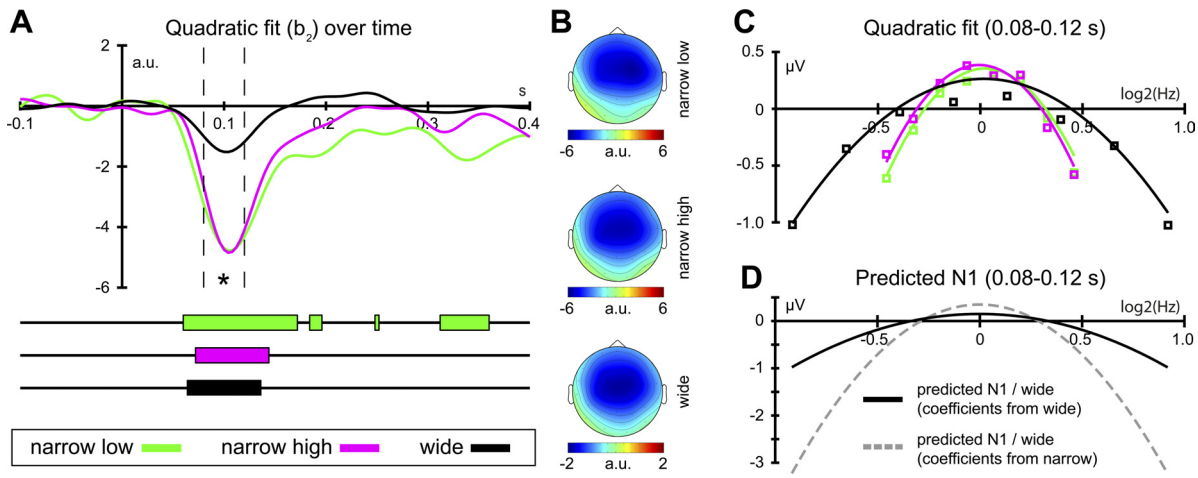

Fig. 4. Results of the quadratic fits (pooled across ignore and attend conditions). *A*: time courses of b_2 coefficients from quadratic fits for each spectral variance condition. Colored horizontal bars below the time courses indicate a significant difference of the b_2 parameter from zero [false discovery rate (FDR) corrected]. *B*: topographical distributions of the b_2 coefficients for the N1 time window (0.08–0.12 s). a.u., Arbitrary units. *C*: mean amplitudes and negative quadratic fits for the N1 time window for each spectral variance condition with their respective tone frequencies in log2-transformed and zero-centered units on the *x*-axis. *D*: predicted N1 for the wide condition. The black solid line indicates N1 amplitudes for the frequencies from the wide spectral variance condition predicted from coefficients estimated for the wide condition. The gray dashed line also shows predicted N1 amplitudes for the wide condition. However, the predictions were made based on coefficients estimated from the narrow spectral variance conditions. The results are inconsistent with a "fixed" spread of adaptation across narrow and wide spectral variance conditions.

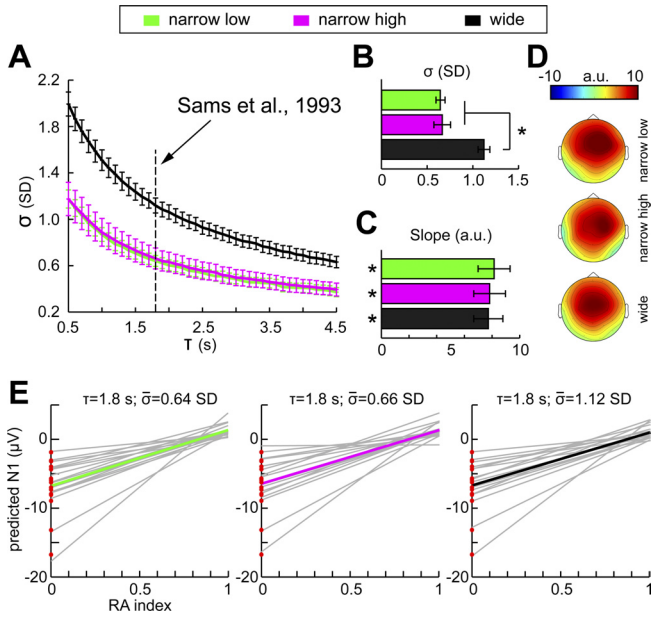

Fig. 5. Estimated adaptation spread of the N1. *A*: mean (±SE) Gaussian width σ describing adaptation spread as a function of τ. The displayed σ values were estimated for each τ independently. The dashed line marks the recovery observed by Sams et al. (1993) ($\tau = 1.8$ s), at which we estimated σ values for statistics. *B*: mean (±SE) σ for each spectral variance condition estimated for the N1 time window. *Significant difference between the wide and narrow conditions. *C*: mean (±SE) slope in the N1 time window for each spectral variance condition given the individual σ at $\tau = 1.8$ s. *Significant difference from zero, i.e., a significant correlation of the N1 amplitude and the RA index. *D*: topographical distributions of the mean slope in the N1 time window for all spectral variance conditions. *E*: predicted N1 amplitudes as a function of RA indices given $\tau = 1.8$ s and individually estimated σ. Mean linear fits are depicted by colored lines and individual fits in gray. Red dots at RA index = 0 reflect the mean N1 amplitudes of the first trials in each block.

eter σ that best describes the brain activations in the N1 time window as a function of the temporal recovery parameter τ.

These results highlight the strong relationship between neural recovery and the spread of adaptation in terms of the contribution to neural response amplitudes. Assuming a longer time period needed for the neural population to recover from previous activation, the spread of adaptation must be tighter in order to explain the single-trial N1 amplitude variations. Similarly, when the neural population recovers more quickly, the spread of adaptation must be broader in order to explain the data. In addition to these observations, Fig. 5, *A* and *B*, also show a clear difference between the adaptation width (σ) in the narrow and wide spectral variance conditions.

For the statistical analysis, a τ of 1.8 s was chosen based on the findings of Sams et al. (1993). The mean best-fit σ values for each spectral variance condition in the N1 time window were as follows: narrow low 0.64 SD (±0.05 SE); narrow high 0.66 SD (±0.09 SE); wide 1.12 SD (±0.06 SE; see Fig. 5, *A* and *B*). Pairwise *t*-tests between conditions did not reveal any differences in the minimized root mean square error of the approximations (for all, $P > 0.25$), indicating comparable goodness of fit in the three spectral variance conditions.

The rmANOVA testing for differences between the σ of the Gaussian (adaptation) function revealed a main effect of spectral variance ($F_{2,30} = 13.11$, $P < 0.001$, $\eta^2_G = 0.064$), caused by broader adaptation spread in the wide condition compared with the narrow conditions (narrow low: $F_{1,15} = 24.55$, $P < 0.001$, $\eta^2_G = 0.066$; narrow high: $F_{1,15} = 14.20$, $P = 0.002$, $\eta^2_G = 0.058$), which were not different from each other ($F_{1,15} = 0.05$, $P = 0.824$).

For each spectral variance condition, slope values (reflecting the correlation between RA indices and N1 amplitude) for individually estimated σ at $\tau = 1.8$ s in the N1 time window were then statistically compared to zero, in order to test whether the RA index is predictive of the single-trial neural activations. The results revealed significant positive slopes in each spectral variance condition (narrow low: $F_{1,15} = 49.74$, $P < 0.001$, $\eta^2_G = 0.435$; narrow high: $F_{1,15} = 46.93$, $P < 0.001$, $\eta^2_G = 0.431$; wide: $F_{1,15} = 53.64$, $P < 0.001$, $\eta^2_G = 0.439$). Thus the lower the RA index the more negative (i.e., larger) the N1 amplitude (Fig. 5, *C* and *E*). The topographical distribution of the slope values showed a centro-frontal maximum (Fig. 5*D*). Moreover, slopes did not differ between spectral variance conditions ($F_{2,30} = 1.14$, $P = 0.319$, $\epsilon = 0.687$).

In other words, these findings show trial-by-trial frequency-specific amplitude modulations of the N1. The RA index predicted these modulations similarly well in all spectral variance conditions. However, the adaptation spread explaining these effects was broadened in the wide condition compared with a tighter adaptation spread in both narrow conditions.

For visualization purposes, Fig. 6*A* depicts single-trial time courses (color-coding polarity of the EEG signal, a so-called "ERP image"; Makeig et al. 2002), sorted as a function of trials' individual RA indices (Fig. 6*C*). Figure 6*B* shows the corresponding amplitude averaged in the N1 time window (delimited by dashed lines in Fig. 6*A*). It is clear that a strong relationship exists between RA indices and single-trial neural activations in the N1 time window.

Finally, in order to test whether the RA index is also predictive of amplitude modulations in other time windows, a linear function was fitted to single-trial amplitudes at each time point as a function of RA indices (for the individual N1-based estimated σ at $\tau = 1.8$ s). Slope values from the linear fits (reflecting the correlation between RA indices and ERP amplitude) were then tested against zero with a *t*-test. The colored horizontal bars below each panel in Fig. *6A* show where the slope values significantly differed from zero (FDR corrected).

Apart from the N1 time window, slopes in the narrow spectral variance conditions were not significantly different from zero in other time windows [i.e., not at all in the P1 time window and for only 2 time samples (0.160–0.164 s) in the P2 time window for the narrow high condition].

In the wide spectral variance condition, slopes were also not significantly different from zero in the P1 time window. However, the RA index correlated negatively with the amplitude in the P2 time window (0.152–0.276 s), that is, the smaller the RA index the more positive (i.e., stronger) the amplitude in the P2 time window in the wide spectral variance condition.

DISCUSSION

The present EEG study investigated the frequency specificity of human auditory cortex responses by randomly presenting tones of different frequencies in rapid sequences that differed in spectral variance. Three main findings are of importance: First, a clear frequency-specific modulation around 100 ms after tone onset was observed for all spectral variance conditions. Second, a simple computational model of frequency-

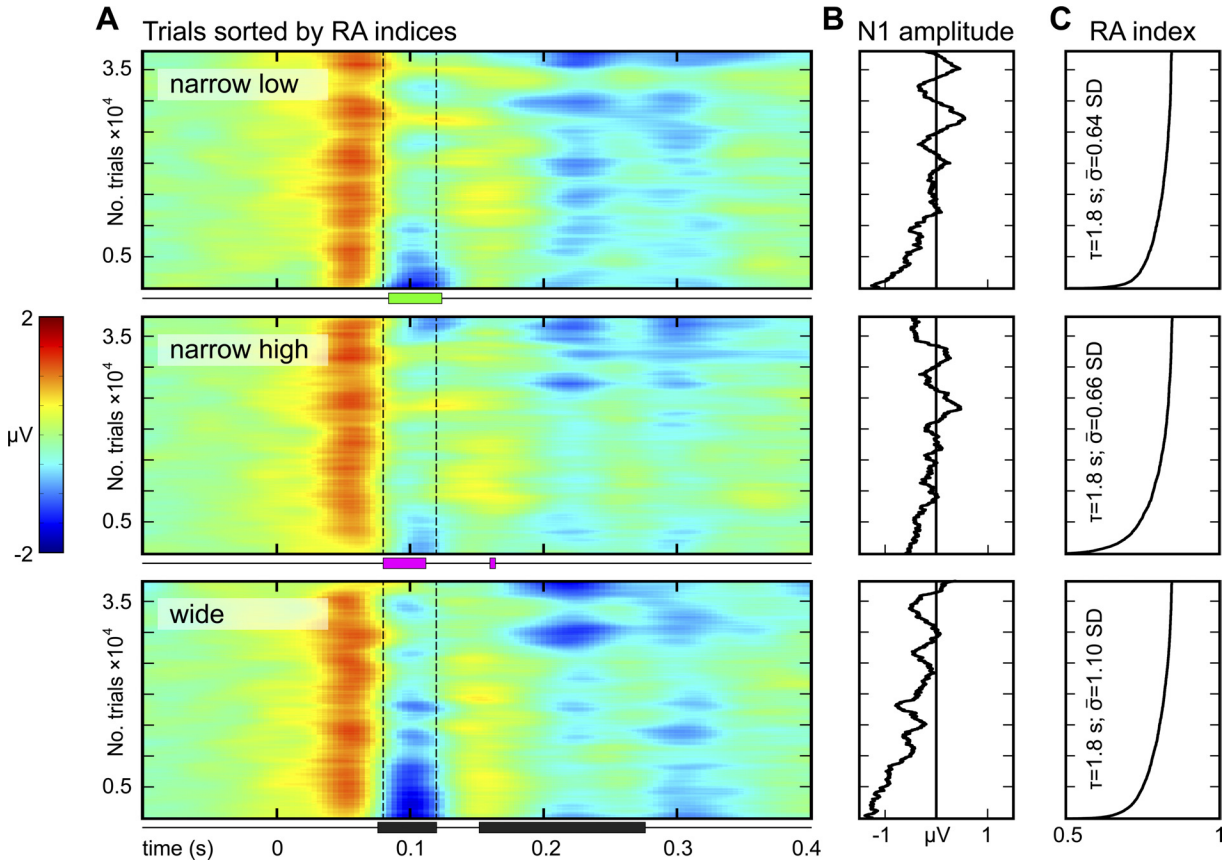

Fig. 6. Single-trial neural activations. *A*: all single-trial time courses (ignore and attend; of all participants) for the 3 spectral variance conditions sorted by the trials' individual RA indices (*C*). Smoothing across trials was applied for visual purposes. Colored horizontal bars below each panel indicate in which time windows slope values (correlation between RA indices and ERP amplitude) differed significantly from zero (FDR corrected). *B*: mean amplitudes in the N1 time window (0.08–0.12 s) extracted from the interval marked by dashed lines in *A*. *C*: sorted single-trial RA indices given $\tau = 1.8$ s and individually estimated σ of the Gaussian adaptation function.

specific adaptation (RA index) based on the spectro-temporal stimulation history adequately predicted single-trial N1 amplitude variations. Third, the spread of adaptation on tonotopically organized regions in auditory cortex depended on the spectral variance in the stimulation. It appeared broadened in the wide compared with the narrow spectral variance conditions.

Frequency specificity of neural responses. A consistent finding in previous studies on frequency specificity in auditory cortex has been an increase in response amplitude (and sometimes a concomitant decrease in response latency) with increasing frequency distance between successive stimuli (Butler 1968; May et al. 1999; Scholl et al. 2008). In line with these studies, mean N1 amplitudes to tone frequencies at the edge of a spectral variance condition were larger than to tone frequencies close to the center frequency (Fig. 3). This is commensurate with a spatial overlap of adapted regions in a tonotopically organized cortical area. Across a block of random tone presentations, regions responding to frequencies distant from the center of the stimulation are affected to a lesser degree than regions responding to frequencies close to the center. In contrast, N1 peak latencies (on average at 103 ms) were unaffected by the frequency spacing between tones.

Furthermore, trial-by-trial auditory cortex amplitude variations were adequately predicted by a simple computational model of response adaptation incorporating adaptation spread and recovery from adaptation over time. This analysis emphasizes that brain responses are strongly dependent on the history of presented tones (cf. Bäuerle et al. 2011; Näätänen et al. 1988; Sams et al. 1993; Ulanovsky et al. 2003, 2004; von der Behrens et al. 2009). Brain responses were smaller when the auditory cortex region corresponding to the presented tone frequency was already highly adapted by preceding tone presentations. The context-dependent nature of auditory cortex responsiveness is also captured by our simple model (Fig. 2) and arguably constitutes an integral part of sensory memory function in audition (Jääskeläinen et al. 2007, 2011).

Neurophysiological mechanisms underlying N1 frequency specificity. The mechanisms underlying the observed frequency-specific N1 amplitude variations and their relation to single-cell behavior, as characterized by spiking activity, are still debated. In the framework of Jääskeläinen et al. (2007, 2011), the phenomenon of reduced response amplitude to a stimulus caused by preceding stimulation is referred to as stimulus-specific adaptation. While they use stimulus-specific adaptation as a conglomerate for a variety of terms discussed in the literature (e.g., adaptation, lateral inhibition, refractoriness, habituation, forward masking, etc.), they consider lateral inhibition specifically to be a neurophysiological mechanism underlying frequency-specific variations of N1 amplitude (Loveless et al. 1989; May et al. 1999). However, from a single-neuron perspective, the present N1 effects occur rather late

(0.08–0.12 s) to reflect lateral inhibition in the classical sense. Hence, there could also be substantial contributions of other inputs, for example, from nonlemniscal pathways (Hu 2003; Tang et al. 2012). In sum, the observed N1 amplitude effects are likely to be multicausal in nature.

In the present study, the estimated adaptation spread is consistent with the proposal that lateral inhibition in auditory cortex spans across several octaves along the tonotopic gradient (May et al. 1999), whereas the tuning width of single neurons can be much smaller (Bartlett et al. 2011; Bitterman et al. 2008). Complicating the picture, the tuning width of neurons widens increasingly along the ascending auditory pathway, and the proportion of sharply tuned neurons decreases (Bartlett et al. 2011). Furthermore, short-term plastic changes might alter neuronal response properties according to the spectral variance in the acoustic stimulation (Bitterman et al. 2008)—a hypothesis strengthened by the present human EEG data (see also next section).

Hence, the present study does not warrant conclusions about whether the frequency-specific N1 amplitude variations directly reflect tuning curve properties of auditory cortex neurons. Also, it cannot rule out effects of lateral inhibition influencing the response properties of regions close to the region responding best to the tone frequency presented.

Short-term plasticity as a mechanism of broadened adaptation spread. Most importantly in the present study, the spread of adaptation in auditory cortex differed between narrow and wide conditions, such that the spread was broadened for tone frequencies spaced widely ("spectral variance"; Fig. 5). This finding of nonfixed frequency specificity reveals an interesting feature of auditory cortex responses coding acoustic stimulations with different spectral variance and might in part explain the diverging observations on adaptation spread reported previously (Butler 1968; Näätänen et al. 1988; Picton et al. 1978).

Frequency-specific adaptation of neural responses highlights the remarkable adjustability of neural populations in auditory cortex. It has been proposed that this short-term plasticity underlies sensory memory functions and is related to a variety of cognitive phenomena (Jääskeläinen et al. 2007, 2011; Ulanovsky et al. 2003). Indeed, short-term plastic adjustment to the spectral variance of the acoustic stimulation might be an efficient sensory memory coding mechanism: It would ensure that wider spectral ranges receive neural coding equally good as that of a narrower spectral range.

Work on short-term plasticity in nonhuman mammals has shown that neurons along the auditory pathway can adjust their response properties to stimulation statistics such as the mean or variance of sounds (Dahmen et al. 2010; Dean et al. 2005; Kvale and Schreiner 2004), and even to more abstract patterns such as the shape of the stimulation distribution (Kvale and Schreiner 2004). Interestingly, short-term plasticity in audition has been proposed to work on postsynaptic potentials (Reyes 2011) and is thus at the very core of what is measured in EEG (Buzsáki et al. 2012). In that sense, our data provide an important missing link between single-cell neurophysiology and human auditory behavior.

In addition, previous EEG studies in humans indicate that tones presented randomly are not perceived as independent entities but rather as a contiguous abstract sound pattern (Rosburg 2004; Wolff and Schröger 2001). Thus coding the history of presented tones in sensory memory into patterns could profit from stimulus-specific adaptation (Jääskeläinen et al. 2007, 2011). At the same time, representing such patterns necessitates the adjustment of neural response properties to the spectral variance of the acoustic stimulation. Accordingly, cell recordings in human auditory cortex revealed that neuronal responses are indeed tuned more broadly to spectrally rich than to spectrally less rich sounds (Bitterman et al. 2008).

Thus we propose the following working hypothesis: Neural response properties in auditory cortex underlie N1 amplitude modulations and subserve sensory memory functions. These response properties are dependent on the history of the acoustic stimulation and, at the same time, adjust flexibly to the spectral variance of the acoustic stimulation. In the present study, spectral variance corresponds to the spacing between tone frequencies as well as to the overall frequency range. Whether neural response properties adjust to changes in stimulus variance on a local scale (i.e., spectral spacing) or on a global scale (i.e., spectral range) is a question that needs to be answered in future research.

Timescale of recovery from adaptation. The present study focused on the degree of adaptation spread (σ) while keeping the recovery time from adaptation (τ) fixed. A constant τ across the narrow and wide conditions was chosen because the onset-to-onset interval in all conditions was fixed at 0.5 s throughout the experiment; only the spectral variance was manipulated. As Fig. 5*A* shows, the effect of broadened adaptation spread in the wide condition would still have been evident even when considering different τ parameters, and thus is not an artifact of our choice of τ.

However, in previous studies investigating recovery from adaptation, the N1 (as recorded in magnetoencephalography, N1m) could be distinguished into two subcomponents. For these N1 subcomponents, different timescales of recovery (i.e., different τ) have been observed (e.g., McEvoy et al. 1997; Sams et al. 1993). Multiple timescales of adaptation have also been reported in individual auditory cortex neurons in anesthetized cats (Ulanovsky et al. 2004). Although we did not observe N1 subcomponents in the present study, the range of τ parameters for which adaptation spread was calculated covered the range of previously observed N1 timescales (Lu et al. 1992b; Mäkelä et al. 1993; McEvoy et al. 1997; Sams et al. 1993). While we consider a change in recovery time rather than adaptation spread unlikely given our experimental setup, it would be an interesting finding in itself if N1 recovery time depended on the spectral properties in the acoustic stimulation.

Frequency specificity of other ERP components. In the present study, P1 amplitudes were not modulated by spectral properties of the tone sequence. This is in contrast to previous studies showing P1 amplitude reduction at comparable onset-to-onset intervals (e.g., Boutros and Belger 1999; Rosburg et al. 2004; Zouridakis and Boutros 1992), where refractoriness has been proposed as an underlying neurophysiological mechanism (Rosburg et al. 2004). Nevertheless, the absence of a P1 effect here emphasizes the functionally different roles of N1 and P1 with respect to frequency specificity.

Note also that such rapid stimulus presentations (onset-to-onset interval of 0.5 s) are usually considered suboptimal for observing N1 responses and more suitable for eliciting P1 responses (see, e.g., Tavabi et al. 2007). Accordingly, N1 responses were smaller in magnitude than P1 responses in the present study, but the adaptation effects occurred in the N1 time window nevertheless.

This suggests that the dynamics of frequency specificity are best investigated when the underlying neural system does not have time to fully recover from adaptation.

In addition, frequency-specific amplitude modulations were observed for the P2, but only in the wide spectral variance condition. This finding might relate to previous observations suggesting weaker frequency specificity of the P2 than N1 component (Picton et al. 1978). Nevertheless, P2 amplitude modulations have been linked to adaptation spanning multiple timescales (Costa-Faidella et al. 2011). Thus there are observations of P2 frequency specificity. However, more research is needed to further examine its dependence on the spectral variance in the stimulation.

Frequency-specific responses were unaffected by attention. Finally, N1 amplitudes were unaffected by whether participants ignored or attended to the stimulation. This is in seeming contrast to previously reported modulations of the N1 under active versus passive listening conditions (e.g., Ahveninen et al. 2011; Hillyard et al. 1973; Okamoto et al. 2007; Schwent et al. 1976).

One possible reason for this apparent discrepancy is that in the present study participants were unable to ignore the stimulation when instructed to do so, and thus may have partially attended to the auditory stimulation in the "ignore" condition. This is highly unlikely, given data from a postexperiment inquiry. Indeed, participants reported high success in how well they were able to ignore the auditory stimulation during ignore blocks (mean rating 3.95, range 2–5, on a 1 to 5 scale).

We consider a more feasible explanation to be that most of the previous studies observing N1 attention effects presented their stimuli at low intensity levels or in background noise (Ahveninen et al. 2011; Hillyard et al. 1973; Okamoto et al. 2007; Schwent et al. 1976). In fact, Schwent et al. (1976) showed that N1 amplitudes for sounds at 60 dB SL and no background noise (current settings) were unaffected by attentive focusing, whereas N1 amplitudes for sounds at 20 dB SL in background noise were different for active versus passive listening. A prediction for future experiments would thus be that the spread of neural adaptation will be affected by attention if noise masking is introduced. This, however, would suggest an interesting interaction between stimulus parameters and attention. At least for suprathreshold stimulation, it is thus safe to conclude for now that sustained attention does not have a strong impact on the adaptation spread in the evoked brain response.

Conclusions. A rapid tone-stimulation paradigm in human EEG combined with simple computational modeling reveals that the spread of frequency-specific adaptation in auditory cortex depends on the context (i.e., the history and variance) of the acoustic stimulation. Spread of adaptation broadens for tone sequences with wide compared with narrow spectral variance, suggesting that auditory cortex response properties are flexibly adjusted to the spectral properties of the acoustic stimulation.

ACKNOWLEDGMENTS

We thank Dunja Kunke for helping with the data acquisition and her technical support in the lab. We further thank Philipp Ruhnau for fruitful discussions in the beginning of this project and three anonymous reviewers for their constructive comments.

GRANTS

The authors are supported by the Max Planck Society (Max Planck Research Group grant to J. Obleser).

DISCLOSURES

No conflicts of interest, financial or otherwise, are declared by the author(s).

AUTHOR CONTRIBUTIONS

Author contributions: B.H. and J.O. conception and design of research; B.H. performed experiments; B.H. and M.J.H. analyzed data; B.H., M.J.H., and J.O. interpreted results of experiments; B.H. prepared figures; B.H. drafted manuscript; B.H., M.J.H., and J.O. edited and revised manuscript; B.H., M.J.H., and J.O. approved final version of manuscript.

REFERENCES

Ahveninen J, Hämäläinen MS, Jääskeläinen IP, Ahlfors SP, Huang S, Lin FH, Raij T, Sams M, Vasios CE, Belliveau JW. Attention-driven auditory cortex short-term plasticity helps segregate relevant sounds from noise. *Proc Natl Acad Sci USA* 108: 4182–4187, 2011.

Bakeman R. Recommended effect size statistics for repeated measures designs. *Behav Res Methods* 37: 379–384, 2005.

Bartlett EL, Sadagopan S, Wang X. Fine frequency tuning in monkey auditory cortex and thalamus. *J Neurophysiol* 106: 849–859, 2011.

Bäuerle P, von der Behrens W, Kössl M, Gaese BH. Stimulus-specific adaptation in the gerbil primary auditory thalamus is the result of a fast frequency-specific habituation and is regulated by the corticofugal system. *J Neurosci* 31: 9708–9722, 2011.

Benjamini Y, Hochberg Y. Controlling the false discovery rate: a practical and powerful approach to multiple testing. *J R Stat Soc Ser B* 57: 289–300, 1995.

Bitterman Y, Mukamel R, Malach R, Fried I, Nelken I. Ultra-fine frequency tuning revealed in single neurons of human auditory cortex. *Nature* 451: 197–201, 2008.

Boutros NN, Belger A. Midlatency evoked potentials attenuation and augmentation reflect different aspects of sensory gating. *Biol Psychol* 45: 917–922, 1999.

Butler RA. Effect of changes in stimulus frequency and intensity on habituation of the human vertex potential. *J Acoust Soc Am* 44: 945–950, 1968.

Buzsáki G, Anastassiou CA, Koch C. The origin of extracellular fields and currents—EEG, ECoG, LFP and spikes. *Nat Rev Neurosci* 13: 407–420, 2012.

Costa-Faidella J, Grimm S, Slabu L, Diaz-Santaella F, Escera C. Multiple time scales of adaptation in the auditory system as revealed by human evoked potentials. *Psychophysiology* 48: 774–783, 2011.

Dahmen JC, Hartley DE, King AJ. Stimulus-timing-dependent plasticity of cortical frequency representation. *J Neurosci* 28: 13629–13639, 2008.

Dahmen JC, Keating P, Nodal FR, Schulz AL, King AJ. Adaptation to stimulus statistics in the perception and neural representation of auditory space. *Neuron* 66: 937–948, 2010.

Dean I, Harper NS, McAlpine D. Neural population coding of sound level adapts to stimulus statistics. *Nat Neurosci* 8: 1684–1689, 2005.

Dean I, Robinson BL, Harper NS, McAlpine D. Rapid neural adaptation to sound level statistics. *J Neurosci* 28: 6430–6438, 2008.

Genovese CR, Lazar NA, Nichols T. Thresholding of statistical maps in functional neuroimaging using the false discovery rate. *Neuroimage* 15: 870–880, 2002.

Gorny JL, Butler RA. An evoked response study of the first-order difference tone in man. *Acta Otolaryngol* 80: 1–6, 1975.

Greenhouse SW, Geisser S. On methods in the analysis of profile data. *Psychometrika* 24: 95–112, 1959.

Hari R, Kaila K, Katila T, Tuomisto T, Varpula T. Interstimulus interval dependence of the auditory vertex response and its magnetic counterpart: implications for their neural generation. *Electroencephalogr Clin Neurophysiol* 54: 561–569, 1982.

Hillyard SA, Hink RF, Schwent VL, Picton TW. Electrical signs of selective attention in the human brain. *Science* 182: 177–180, 1973.

Hu B. Functional organization of lemniscal and nonlemniscal auditory thalamus. *Exp Brain Res* 153: 543–549, 2003.

Jääskeläinen IP, Ahveninen J, Andermann ML, Belliveau JW, Raij T, Sams M. Short-term plasticity as a neural mechanism supporting memory and attentional functions. *Brain Res* 1422: 66–81, 2011.

Jääskeläinen IP, Ahveninen J, Belliveau JW, Raij T, Sams M. Short-term plasticity in auditory cognition. *Trends Neurosci* 30: 653–661, 2007.

Kvale MN, Schreiner CE. Short-term adaptation of auditory receptive fields to dynamic stimuli. *J Neurophysiol* 91: 604–612, 2004.

Leek MR. Adaptive procedures in psychophysical research. *Percept Psychophys* 63: 1279–1292, 2001.

Loveless N, Hari R, Hämäläinen MS, Tiihonen J. Evoked responses of human auditory cortex may be enhanced by preceding stimuli. *Electroencephalogr Clin Neurophysiol* 74: 217–227, 1989.

Lu ZL, Williamson SJ, Kaufman L. Behavioral lifetime of human auditory sensory memory predicted by physiological measures. *Science* 258: 1688–1670, 1992a.

Lu ZL, Williamson SJ, Kaufman L. Human auditory primary and association cortex have differing lifetimes for activation traces. *Brain Res* 572: 236–241, 1992b.

Maess B, Jacobsen T, Schröger E, Friederici AD. Localizing pre-attentive auditory memory-based comparison: magnetic mismatch negativity to pitch change. *Neuroimage* 37: 561–571, 2007.

Makeig S, Westerfield M, Jung TP, Enghoff S, Townsend J, Courchesne E, Sejnowski TJ. Dynamic brain sources of visual evoked responses. *Science* 295: 690–694, 2002.

Mäkelä JP, Ahonen A, Hämäläinen MS, Hari R, Ilmoniemi RJ, Kajola M, Knuutila J, Lounasmaa OV, McEvoy L, Salmelin R, Salonen O, Sams M, Simola J, Tesche C, Vasama JP. Functional differences between auditory cortices of the two hemispheres revealed by whole-head neuromagnetic recordings. *Hum Brain Mapp* 1: 48–56, 1993.

May PJ, Tiitinen H, Ilmoniemi RJ, Nyman G, Taylor JG, Näätänen R. Frequency change detection in human auditory cortex. *J Comput Neurosci* 6: 99–120, 1999.

McEvoy L, Levänen S, Loveless N. Temporal characteristics of auditory sensory memory: neuromagnetic evidence. *Psychophysiology* 34: 308–316, 1997.

Montgomery N, Wehr M. Auditory cortical neurons convey maximal stimulus-specific information at their best frequency. *J Neurosci* 30: 13362–13366, 2010.

Näätänen R, Picton TW. The N1 wave of the human electric and magnetic response to sound: a review and an analysis of the component structure. *Psychophysiology* 24: 375–425, 1987.

Näätänen R, Sams M, Alho K, Paavilainen P, Reinikainen K, Sokolov EN. Frequency and location specificity of the human vertex N1 wave. *Electroencephalogr Clin Neurophysiol* 69: 523–531, 1988.

Okamoto H, Stracke H, Wolters CH, Schmael F, Pantev C. Attention improves population-level frequency tuning in human auditory cortex. *J Neurosci* 27: 10383–10390, 2007.

Oldfield RC. The assessment and analysis of handedness: the Edinburgh Inventory. *Neuropsychologia* 9: 97–113, 1971.

Oostenveld R, Fries P, Maris E, Schoffelen JM. FieldTrip: open source software for advanced analysis of MEG, EEG, and invasive electrophysiological data. *Comput Intell Neurosci* 2011: Article ID 156869, 2011.

Pantev C, Hoke M, Lehnertz K, Lütkenhöner B, Anogianakis G, Wittkowski W. Tonotopic organization of the human auditory cortex revealed by transient auditory evoked magnetic fields. *Electroencephalogr Clin Neurophysiol* 69: 160–170, 1988.

Picton TW, Woods DL, Proulx GB. Human auditory sustained potentials. II. Stimulus relationships. *Electroencephalogr Clin Neurophysiol* 45: 198–210, 1978.

Reyes AD. Synaptic short-term plasticity in auditory cortical circuits. *Hear Res* 279: 60–66, 2011.

Rosburg T. Effects of tone repetition on auditory evoked neuromagnetic fields. *Clin Neurophysiol* 115: 898–905, 2004.

Rosburg T, Trautner P, Korzyukov OA, Boutros NN, Schaller C, Elger CE, Kurthen M. Short-term habituation of the intracranially recorded auditory evoked potentials P50 and N100. *Neurosci Lett* 372: 245–249, 2004.

Rosburg T, Zimmerer K, Huonker R. Short-term habituation of auditory evoked potential and neuromagnetic field components in dependence of the interstimulus interval. *Exp Brain Res* 205: 559–570, 2010.

Sams M, Hari R, Rif J, Knuutila J. The human auditory sensory memory trace persists about 10 sec: neuromagnetic evidence. *J Cogn Neurosci* 5: 363–370, 1993.

Scholl B, Gao X, Wehr M. Level dependence of contextual modulation in auditory cortex. *J Neurophysiol* 99: 1616–1627, 2008.

Schwent VL, Hillyard SA, Galambos R. Selective attention and the auditory vertex potential. II. Effects of signal intensity and masking noise. *Electroencephalogr Clin Neurophysiol* 40: 615–622, 1976.

Smulders FT. Simplifying jackknifing of ERPs and getting more out of it: retrieving estimates of participants' latencies. *Psychophysiology* 47: 387–392, 2010.

Studebaker GA. A "rationalized" arcsine transform. *J Speech Hear Res* 28: 455–462, 1985.

Taaseh N, Yaron A, Nelken I. Stimulus-specific adaptation and deviance detection in the rat auditory cortex. *PloS One* 6: e23369, 2011.

Tang J, Yang W, Suga N. Modulation of thalamic auditory neurons by the primary auditory cortex. *J Neurophysiol* 108: 935–942, 2012.

Tavabi K, Obleser J, Dobel C, Pantev C. Auditory evoked fields differentially encode speech features: an MEG investigation of the P50m and N100m time courses during syllable processing. *Eur J Neurosci* 25: 3155–3162, 2007.

Ulanovsky N, Las L, Farkas D, Nelken I. Multiple time scales of adaptation in auditory cortex neurons. *J Neurosci* 24: 10440–10453, 2004.

Ulanovsky N, Las L, Nelken I. Processing of low-probability sounds by cortical neurons. *Nat Neurosci* 6: 391–398, 2003.

von der Behrens W, Bäuerle P, Kössl M, Gaese BH. Correlating stimulus-specific adaptation of cortical neurons and local field potentials in the awake rat. *J Neurosci* 29: 13837–13849, 2009.

Wolff C, Schröger E. Activation of the auditory pre-attentive change detection system by tone repetitions with fast stimulation rate. *Cogn Brain Res* 10: 323–327, 2001.

Zouridakis G, Boutros NN. Stimulus parameter effects on the P50 evoked response. *Biol Psychiatry* 32: 839–841, 1992.